DOI: 10.1002/chem.200800029

On the Mechanisms of Degenerate Ligand Exchange in $[M(CH_3)]^+/CH_4$ Couples (M = Fe, Co, Ni, Ru, Rh, Pd, Os, Ir, Pt) as Explored by Mass Spectrometric and Computational Studies: Oxidative Addition/Reductive Elimination versus σ-Complex-Assisted Metathesis

Marc Armélin, Maria Schlangen, and Helmut Schwarz*[a]

Dedicated to Professor Klaus Hafner on the occasion of his 80th birthday

Abstract: The degenerate ligand exchange in $[M(CH_3)]^+/CH_4$ couples occurs in the gas phase at room temperature for M = Ni, Ru, Rh, Pd, and Pt, whereas the complexes containing Fe and Co are unreactive. Details of hydrogen-atom scrambling versus direct ligand switch have been uncovered by labeling experiments with CD_4 and $^{13}CH_4$, respectively. The reactivity scale ranges from unreactive (M = Fe, Co) or inefficient (M = Ni, Pd) to moderately (M = Ru) and rather reactive (M = Rh, Pt). Quite extensive, but not complete, H/D exchange between the hydrogen atoms of the incoming and outgoing methyl groups is observed for M = Pt, whereas for M = Ni and Pd a predominantly direct ligand switch prevails. DFT calculations performed at the B3LYP level of theory account well for the thermal nonreactivity of the Fe and Co couples. For $[Ni[CH_3)]^+/CH_4$, a σ-complex-assisted metathesis (σ-CAM) is operative such that, in a two-state reactivity (TSR) scenario, two spin flips between the ^{3}A ground and ^{1}A excited states take place at the entrance and exit channels of the encounter complexes. For M = Ru and Rh, only oxidative addition/reductive elimination (OA/RE) is favored energetically, and the reaction is confined to the electronic ground states ^{3}A and ^{2}A. In contrast, for the $[Pd(CH_3)]^+/CH_4$ system, on the ^{1}A ground-state potential-energy surface both the OA/RE and σ-CAM variants are energetically comparable, and the small reaction efficiency for the ligand switch is reflected in transition states located energetically close to the reactants. For the $[M(CH_3)]^+/CH_4$ complexes of the 5d elements, the σ-CAM mechanism does not play a role. For M = Pt, the energetically most favored path proceeds in a spin-conserving manner on the ^{1}A potential-energy surface, which accounts for the extensive single and double hydrogen-atom exchange preceding ligand exchange. Although for M = Os and Ir the $[M(CH_3)]^+$ complexes could not be generated experimentally, computational studies predict that both systems may undergo thermal reaction with CH_4, and an OA/RE mechanism will commence on the respective high-spin ground states; however, the bond-activation and ligand-exchange steps will occur on the excited low-spin surfaces in a TSR scenario.

Keywords: ligand exchange · metathesis · methane · reaction mechanisms · transition metals

Introduction

The commonly invoked mechanisms for transition-metal-mediated C–H bond activation include oxidative addition/reductive elimination (OA/RE) and σ-bond metathesis (σ-BM; Scheme 1). Although the latter is typical for d^0 metals and requires no intermediates, the former is inherently a multistep reaction and is associated with a change of formal oxidation states. Examples of OA/RE processes often include complexes of electron-rich, late transition metals.[1] More recently, quite a few systems surfaced in which late-transition-metal complexes were reported to bring about, for example, isotope exchange without exhibiting the features characteristic of an OA/RE reaction.[2] Therefore, based on experimental data and computational studies, a mechanistic variant was suggested in which σ complexes undergo a metathesis process, and the term σ-complex-assisted metathesis (σ-CAM) has been introduced to distinguish the

[a] M. Armélin, M. Schlangen, Prof. Dr. H. Schwarz
Institut für Chemie, Technische Universität Berlin
Strasse des 17 Juni 135, 10623 Berlin (Germany)
Fax: (+49) 30-3142-1102
E-mail: Helmut.Schwarz@mail.chem.tu-berlin.de

Supporting information for this article is available on the WWW under http://www.chemeurj.org/ or from the author.

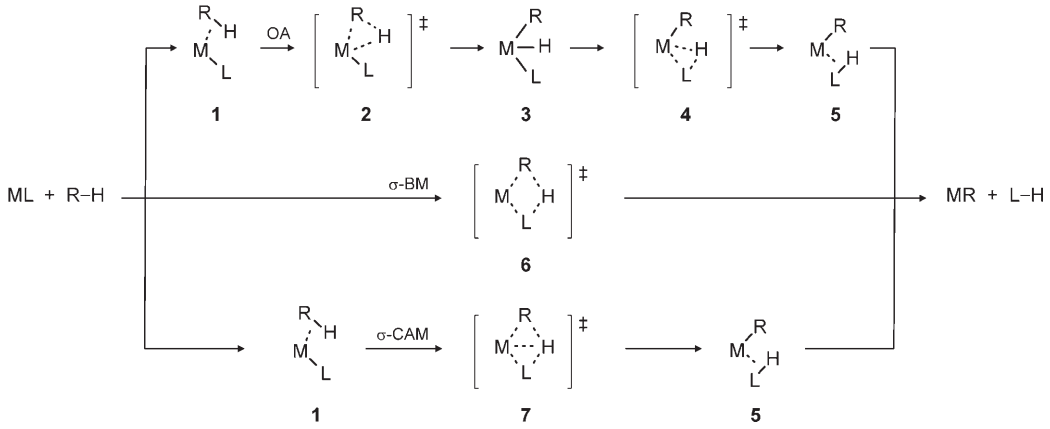

Scheme 1. Mechanistic variants for transition-metal (ML)-mediated C–H bond activation of hydrocarbons RH: oxidative addition/reductive elimination (OA/RE), σ-bond metathesis (σ-BM), and σ-complex-assisted metathesis (σ-CAM).

route **1**→**7**→**5** from a direct four-center σ-BM rearrangement proceeding through **6** (Scheme 1).

Although attempted distinctions of mechanistic variants may be reminiscent of numerous, occasionally semantic, debates about the role of concepts in chemistry or the nature of chemical bonding,[3] technical distinctions seem to exist and demarcation into categories can be useful provided one does not forget that the "real" mechanism may well lie in a continuum defined by the extremes of these classifications.[2,4]

A good example to underline the mechanistic manifold operative in formally similar processes concerns the recently reported thermal activation of methane by group 10 metal hydrides $[MH]^+$ [Eq. (1)].

$$[MH]^+ + CH_4 \longrightarrow [M(CH_3)]^+ + H_2 \quad (1)$$

(M = Ni, Pd, Pt)

Although the reactions of these diatomic $[MH]^+$ ions with methane have many features in common,[5] fundamental differences exist with regard to the details of the potential-energy surfaces (PESs) and thus to the actual reaction mechanisms. As shown by Zhang and Bowers,[5c] the Ni-mediated H/CH_3 ligand exchange constitutes a textbook example of the operation of "two-state reactivity" (TSR)[6] because crossings between the high-spin and low-spin surfaces take place at both the entrance and exit channels of reaction (1) (M = Ni). Thereby, a pathway is opened up that avoids an energetically rather unfavorable transition structure associated with a spin-conserving σ-metathesis process on the high-spin ground-state surface. This TSR scenario is favored by the relatively small energy separation ($<100\,kJ\,mol^{-1}$) of the two relevant spin states of NiH^+, that is, ground state $^3\Delta$ and excited $^1\Sigma^+$. In distinct contrast, the $[PdH]^+/CH_4$ couple can be fully explained without invoking a multistate pattern. As the excited states of $[PdH]^+$ ($^3\Delta$ and $^3\prod$) are $>320\,kJ\,mol^{-1}$ higher in energy than the $^1\Sigma^+$ ground state, they are too high in energy to contribute to a TSR scenario; instead, the whole reaction proceeds on the singlet PES in a spin-conserving manner. However, based on DFT calculations in reaction (1), both the OA/RE and σ-CAM mechanisms are indistinguishable energetically.[5f] Finally, for the $[PtH]^+/CH_4$ system, one encounters yet another electronic and mechanistic situation. Here, the $^1\Sigma^+$ and $^3\Delta$ states are practically isoenergetic[7] and, as spin–orbit coupling for heavy elements is generally rather efficient,[8] a multitude of both single- and multistate reactivity routes are accessible in the course of the platinum-mediated H/CH_3 ligand exchange. Obviously, for the three formally related group 10 metal-hydride cations in their thermal reaction with methane and with regard to the mechanistic details, it is deemed appropriate to employ the phrase "*the same and not the same*" coined by R. Hoffmann in a different context.[9] Furthermore, based on theoretical considerations, a continuum of mechanisms has also been suggested for the condensed-phase reactions of methane with various organometallic complexes including the transition metals Fe, Ru, Rh, Pd, Os, Ir, and Pt.[4c,10]

Herein, we describe the degenerate ligand exchange of seven late-transition-metal complexes with methane [Eq. (2)] in the gas phase. To this end, $[M(CH_3)]^+$ ions were generated by different means (see Experimental Section), mass-selected, and reacted at room temperature with CD_4 and $^{13}CH_4$. The experimental findings were compared with DFT-based computational studies in the hope of revealing the mechanisms operative in these thermoneutral ligand-exchange processes. Combined experimental/theoretical investigations of this type have been implicated and suggested as appropriate models for probing qualitatively the mechanistic aspects of the scenario depicted in Scheme 1.[2,4] Although there have been numerous computational attempts to generalize bond-activation mechanisms in terms of spin-state features,[5a,f,6,7] a systematic approach for describing coherently a set of related reactions, for example, degenerate ligand exchange processes, has not yet been reported [Eq. (2)].

$$[M(CH_3)]^+ + CD_4 \longrightarrow [M(CH_{3-x}D_x)]^+ + CD_{4-x}H_x \quad (2a)$$

(M = Fe, Co, Ni, Ru, Rh, Pd, Pt) ($x = 1-3$)

$$[M(CH_3)]^+ + {}^{13}CH_4 \longrightarrow [M({}^{13}CH_3)]^+ + CH_4 \quad (2b)$$

(M = Rh, Pd, Pt)

Experimental and Computational Details

In the present gas-phase studies two different mass spectrometry-based techniques were employed.[11] In one set of experiments a Spectrospin CMS 47X Fourier transform ion cyclotron resonance (FTICR) mass spectrometer[12] equipped with a Smalley-type[13] cluster-ion source[14] was used. In brief, the beam of a pulsed Nd:YAG laser operating at 1064 nm is focused on a rotating pure metal target to generate a hot metal plasma entrenched in helium to bring about (partial) thermalization. After transfer of the thus-produced ions to the ICR cell by means of a set of electrostatic potentials and lenses, the cationic species of interest are mass-selected using the FERETS ion-ejection protocol,[15] collisionally thermalized, and reacted by pulsing-in a mixture of methyl iodide and argon (1:2 ratio) to generate $[M(CH_3)]^+$ ions, according to Equation (3).

$$M^+ + CH_3I \longrightarrow [M(CH_3)]^+ + I^\bullet \quad (3)$$

For M = Fe, Co, and Pt the formation of the cationic metal–methyl complexes is exothermic[16] and does occur; for the other transition-metal cations this route fails because the reaction is either endothermic, hindered by a barrier or, as for palladium, the transiently produced $[Pd(CH_3)]^+$ cation undergoes an extremely efficient secondary reaction with the substrate [Eq. (4)][17]:

$$[Pd(CH_3)]^+ + CH_3I \longrightarrow [Pd(CH_2I)]^+ + CH_4 \quad (4)$$

thus preventing the buildup of sufficiently large concentrations of $[Pd(CH_3)]^+$ for probing the ligand exchange according to Equation (2).

For iridium, yet another problem was encountered. Although atomic Ir^+ reacts with CH_3I upon expulsion of $I^\bullet$, the resulting cationic product has the structure of an iridium hydride carbene complex $[Ir(H)(CH_2)]^+$, as evidenced by collision-induced dissociation (CID) experiments and ion–molecule reactions. Finally, for osmium all attempts so far have failed to produce the required $[Os(CH_3)]^+$ ion.

For probing the ligand exchange, the mass-selected and thermalized $[M(CH_3)]^+$ ions were subjected to ion–molecule reactions with leaked-in CD_4 at stationary pressures of the order of 10^{-8} mbar. The experimental second-order rate constants k are evaluated on the basis of the pseudo-first-order approximation with an absolute error of $\pm 30\%$;[18] ion-gauge sensitivities[19] and calibration factors[18] were taken into account. The reaction efficiencies ϕ_{rel} are given relative to the $[Pt(CH_3)]^+/CH_4$ system, which itself has an absolute efficiency of 2% when expressed by the ratio of the bimolecular rate constant k and the rate constant derived from the average dipole orientation (ADO) approach.[18,20]

Except for Ir^+ and Os^+, some of the $[M(CH_3)]^+$ complexes that could not be generated by reacting atomic M^+ with CH_3I in the FTICR experiments were produced by ESIMS using a commercial VG BIO-Q mass spectrometer with QHQ configuration (Q: quadrupole, H: hexapole) equipped with an ESI source, as described in detail previously.[21] In brief, the $[M(CH_3)]^+$ ions were formed from millimolar solutions of metal halides in methanol or ethanol, respectively, under relatively harsh ionization conditions (typical cone voltages were around 70–100 V).[22] After mass selection by Q1, the thermalized $[M(CH_3)]^+$ ions (identified by their characteristic isotope pattern and by CID experiments) were exposed to react with CD_4 or $^{13}CH_4$ admitted to the hexapole collision cell at room temperature and at pressures on the order of 10^{-4} mbar; this pressure regime is considered to correspond to nearly single-collision conditions. Ionic products were analyzed by using Q2. The ion-reactivity studies were performed at an interaction energy in the hexapole nominally set to 0 eV.[5d,23] With these two techniques, except for M = Os and Ir, all other group 8–10 transition-metal complexes $[M(CH_3)]^+$ could be generated and studied experimentally.[11]

In the computational exercise the geometries of all species were optimized at the B3LYP level of theory,[24] as implemented in the Gaussian 03 program package[25] using basis sets of approximately triple-ξ quality. For H and C atoms these were the triple-ξ plus polarization basis sets (TZVP) of Ahlrichs and co-workers,[26] and for Fe, Co, and Ni atoms the TZVP basis sets were augmented by f functions as developed by Wachters.[27] For the transition metals Ru, Rh, Pd, Os, Ir, and Pt, the Stuttgart–Dresden scalar relativistic pseudopotentials were employed in conjunction with the corresponding basis sets.[28]

The nature of the stationary structures as minima or saddle points was characterized by frequency analysis, and intrinsic reaction coordinate (IRC) calculations were performed to link transition structures with the intermediates shown.[29] Relative energies (given in kJ mol^{-1}) are corrected for unscaled zero-point vibrational energy contributions; bond lengths are given in Ångstroms and angles in degrees.

Results and Discussion

We will proceed in three steps. First, the relative efficiencies ϕ_{rel} of the degenerate ligand exchange for the $[M(CH_3)]^+/CH_4$ couples will be presented (Table 1); this is followed by a discussion of the labeling experiments (Table 2). Finally, the experimental findings will be contrasted and compared with the outcome of the computational studies (Table 3, Figures 1, 2, and 3). In the latter, we will also include a brief

analysis of the $[Ir(CH_3)]^+$ and $[Os(CH_3)]^+$ systems, although they could not be investigated experimentally.

As shown in Table 1, the $[M(CH_3)]^+$ ions of the third-row, late-transition-metal cations Fe^+ and Co^+ do not undergo thermal ligand exchange with methane, that is, their rate constants must be $<10^{-14}$ cm^3 molecule^{-1} s^{-1}. For the $[Ni(CH_3)]^+/CH_4$ couple, however, the ligand switch occurs with a relative efficiency that is rather small ($\phi_{rel}=7\%$). These observations are somehow analogous to the behavior of the related $[MH]^+/CH_4$ systems [Eq. (1)], which also exhibit a significantly higher reactivity for the nickel complex compared to those containing iron and cobalt.[5c] In contrast to the complexes of the 3d metal ions, the 4d analogues possess higher reactivities for $[Ru(CH_3)]^+$ and $[Rh(CH_3)]^+$ but, surprisingly, a rather modest efficiency of only $\phi_{rel}=2\%$ for palladium. Finally, the $[Pt(CH_3)]^+/CH_4$ couple undergoes ligand exchange with the highest efficiency ($\phi=2\%$ in terms of ADO).

Table 1. Rate constants (k) and relative reaction efficiencies (ϕ_{rel}) for the degenerate ligand exchange in $[M(CH_3)]^+/CH_4$ couples.

$[M(CH_3)]^+$	k [cm^3 molecule^{-1} s^{-1}]	ϕ_{rel}[b] [%]
Fe	[a]	–
Co	[a]	–
Ni	1.6×10^{-12}	7
Ru	5.1×10^{-12}	23
Rh	1.6×10^{-11}	72
Pd	4.4×10^{-13}	2
Pt	2.2×10^{-11}[c]	100

[a] No thermal reaction observed at the detection limit. [b] Relative to M = Pt with $\phi_{rel}=100\%$. [c] This corresponds to $\phi=2\%$ in terms of ADO.

Some insight into the course of the reactions is provided by labeling experiments (Table 2). Irrespective of their quite varying efficiencies, for the complexes with M = Ni, Ru, Rh, and Pd the contribution of a direct ligand exchange $CH_3 \rightarrow CD_3$ is rather high; nevertheless, single and some double hydrogen/deuterium-atom exchange between the incoming and outgoing methyl groups precedes the actual ligand switch. In contrast, for the Pt system the fraction of direct ligand exchange is negligible. Instead, the labeling data reveal extensive single, double, and even some triple H/D exchange without reaching a complete scrambling of all seven hydrogen/deuterium atoms. Interestingly, extensive H/D exchange has also been reported for the Pt^+-based methane activation in solution.[30] A quantitative analysis of the individual contributions of direct ligand exchange, hydrogen/deuterium scrambling, and the possible operation of kinetic isotope effects is not meaningful for the systems investigated given the limited set of data available.[22b,31] For the $[M(CH_3)]^+$ ions with M = Rh, Pd, and Pt, thermal reactions with $^{13}CH_4$ have been performed as well. These three complexes were chosen on the grounds that they cover systems that exhibit low (M = Pd), intermediate (M = Rh), and higher (M = Pt) reaction efficiencies and—with regard to the competition of hydrogen-atom scrambling versus direct exchange—encompass scenarios of very extensive H/D exchange (M = Pt) as well as high contributions of a direct ligand switch (M = Pd, Rh). Without any exception, the occurrence of the thermal exchange process [Eq. (2b)] has been verified, and for M = Rh and Pd the reaction efficiencies are comparable to those measured for their deuterated analogues, whereas for the $[Pt(CH_3)]^+/^{13}CH_4$ system we note a drop in reactivity. This finding is in line with the hydrogen/deuterium scrambling results, which are rather extensive for the $[Pt(CH_3)]^+/CD_4$ couple, thus demonstrating the operation of a set of forward/backward reactions; of course, these do not show up in the experiment with $^{13}CH_4$.[31d] Finally, from Table 2 we note a very close labeling distribution for the $[Pt(CH_3)]^+/CD_4$ couple irrespective of the mode of $[M(CH_3)]^+$ formation, that is, through reacting atomic M^+ with CH_3I (FTICR) or generation from solutions of platinum halides in CH_3OH (ESI); this finding suggests that we are probing the inherent features of the reactions. If there are any internal energy effects, at least for the present case, they are not significant.

Table 2. Deuterium distribution in the degenerate ligand exchange according to Equation (2a).

Precursor ion	Product ions[a,b]		
$[M(CH_3)]^+$	$[M(CH_2D)]^+$	$[M(CHD_2)]^+$	$[M(CD_3)]^+$
Ni	27	12	61
Ru	37	24	39
Rh	30	35	35
Pd	11	2	87
Pt	41 (42)[c]	42 (45)[c]	16 (13)[c]

[a] Expressed in %. [b] For a complete scrambling of three hydrogen and four deuterium atoms, ignoring kinetic isotope effects, after renormalization one expects for the $[M(CH_{3-x}D_x)]^+$ ($x=1$–3) signals a ratio of 12:53:35. [c] For the $[Pt(CH_3)]^+/CD_4$ couple experiments were conducted using FTICR and ESIMS. The numbers in parentheses refer to the latter.

In Table 3 the relative energies, based on B3LYP calculations, are given for all nine $[M(CH_3)]^+/CH_4$ couples in their two lowest electronic spin states. Except for $Ru(CH_3)^+$, the assignments for the most stable spin state concur with previous theoretical studies performed at higher levels of theory.[32] In these previous, detailed investigations, in addition to making a comparison of computational methods, the focus was on a rigorous description of the electronic structures and the energetic features of $[M(CH_3)]^+$ ions; mechanistic aspects, as depicted in Scheme 1, were not addressed. As the reaction profiles of the degenerate ligand exchange are symmetrical, for the sake of clarity we only include one half of the profiles; for illustrative purposes, for the three systems their two-dimensional half-reaction profiles are depicted in Figures 1–3 (the notation used refers to Scheme 1). In view of the fact that gas-phase ion–molecule processes of the type considered here by definition proceed through encounter complexes, the *direct* σ-metathesis process, involving transition structure **6**, has not been addressed in the computational studies. Rather, the focus is on a comparison of the OA/RE versus the σ-CAM variants. Finally, the geometrical details of all species considered are available as Supporting Information; only a few structural aspects that are indicative

Table 3. B3LYP-calculated relative energies [kJ mol^{-1}] for the degenerate ligand exchange $[M(CH_3)]^+ + {}^*CH_4 \rightleftarrows [M({}^*CH_3)]^+ + CH_4$.[a]

	Intermediates/transition structures			
$[M(CH_3)]^+/CH_4$	**1**	**2**	**3**	**7**
$[Fe(CH_3)]^+$ ^{5}A	0	−61	[b]	[b]	122
$[Fe(CH_3)]^+$ ^{3}A	90	25	117	116	118
$[Co(CH_3)]^+$ ^{4}A	0	−62	[b]	[b]	128
$[Co(CH_3)]^+$ ^{2}A	88	−8	[c]	101	75
$[Ni(CH_3)]^+$ ^{3}A	0	−65	[b]	[b]	91
$[Ni(CH_3)]^+$ ^{1}A	73	−22	41	38	28
$[Ru(CH_3)]^+$ ^{3}A[d]	0	−71	−40	−69	−21
$[Ru(CH_3)]^+$ ^{5}A[d]	9	−68	[c]	85	124
$[Rh(CH_3)]^+$ ^{2}A	0	−76	−39	−45	[e]
$[Rh(CH_3)]^+$ ^{4}A	13	−36	[c]	109	118
$[Pd(CH_3)]^+$ ^{1}A	0	−59	−2	−17	9
$[Pd(CH_3)]^+$ ^{3}A	87	29	[c]	145	77
$[Os(CH_3)]^+$ ^{5}A	0	−33	40	25	[e]
$[Os(CH_3)]^+$ ^{3}A	116	−30	−19	−119	[e]
$[Ir(CH_3)]^+$ ^{4}A	0	−48	[c]	19	[e]
$[Ir(CH_3)]^+$ ^{2}A	42	−68	−52	−154	[e]
$[Pt(CH_3)]^+$ ^{1}A	0	−114	−96	−194	[e]
$[Pt(CH_3)]^+$ ^{3}A	2	−49	25	12	[e]

[a] Energies are given relative to the separated reactant couples $[M(CH_3)]^+/CH_4$. For each metal complex, the relative energies refer to the ground state of $[M(CH_3)]^+$. For the structural assignments, see Scheme 1 and text. [b] Transition state **2** and insertion product **3** have not been located. [c] Transition state **2** has not been located. [d] According to reference [32b], the quintet state corresponds to the electronic ground-state configuration. [e] Transition state **7** has not been located.

of the mechanisms under consideration are included. Even though the accuracy of the energetic data provided by DFT calculations should not be overestimated,[33] the results obtained provide interesting and useful *qualitative* insight into the mechanistic issues described in the Introduction.

The experimental observation that the 3d metal complexes of $[Fe(CH_3)]^+$ and $[Co(CH_3)]^+$ do not react thermally with CH_4 can be accounted for by the computed energetics. For the ^{5}A ground state of $[Fe(CH_3)]^+$, the transition state for a σ-CAM reaction is located 122 kJ mol^{-1} above the entrance channel. All attempts to map out an OA/RE process failed in that they resulted in geometries typical for a σ-CAM mechanism. Consideration of the ^{3}A excited state does not improve the energetically unfavorable situation, because both mechanistic pathways are so demanding in energy that they are not accessible thermally either. The $[Co(CH_3)]^+/CH_4$ couple exhibits a similar pattern in that for the ^{4}A ground state the σ-CAM path requires 128 kJ mol^{-1}, and an OA/RE variant, once more, does not exist for this high-spin system. For the excited ^{2}A state, the transition state of a σ-CAM path is located below the entrance channel of the low-spin system as well as the σ-CAM transition state of the ground-state high-spin electromer, thus indicating a possible TSR scenario.[6] However, the calculated energy demand of 75 kJ mol^{-1}, relative to the entrance point of the electronic ^{4}A ground state, is still much too high to bring about a thermal ligand switch. For the $[Ni(CH_3)]^+/CH_4$ system, the situation is qualitatively reminiscent of that for $[Co(CH_3)]^+/CH_4$ in that on the ^{3}A high-spin ground-state surface, the adiabatic ligand exchange through a σ-CAM transition state is rather high in energy (91 kJ mol^{-1}) and the OA/RE variant does not exist. Whereas for an OA/RE path a transition state was found for the low-spin ^{1}A surface, the transition state for a σ-CAM mechanism is at 28 kJ mol^{-1}, about 13 kJ mol^{-1} lower in energy and only slightly above the ground-state entrance channel. If this computed number is realistic, some thermal energy of the reactants is required to surmount the transition-state barrier. Thus, in a TSR scenario (Figure 1) with spin flips at both the entrance and exit channels, the high-energy transition state of the ^{3}A ground-state PES can be bypassed; this variant accounts for the inefficient, but experimentally clearly detectable, ligand exchange. Although there are some quantitative differences, the behavior of the third-row complexes $[M(CH_3)]^+$ (M = Fe, Co, Ni) towards methane expresses features that were noted earlier for the related $[MH]^+/CH_4$ couples [Eq. (1)], in that for the latter it was also the $[NiH]^+/CH_4$ system that exhibited the highest reactivity due to an energetically favorable TSR pattern involving a σ-CAM mechanism.[5c]

The $[M(CH_3)]^+$ complexes of the 4d transition metals M = Ru, Rh, and Pd differ in several interesting and somehow surprising aspects from their 3d congeners. As stated earlier in a different context,[7a,b] their electronic ground states prefer low-spin configurations[32b] and are thus more prone to OA/RE reactions than the high-spin electromers. In fact, in line with the experimental findings (Table 1), all three complexes bring about thermal methyl ligand ex-

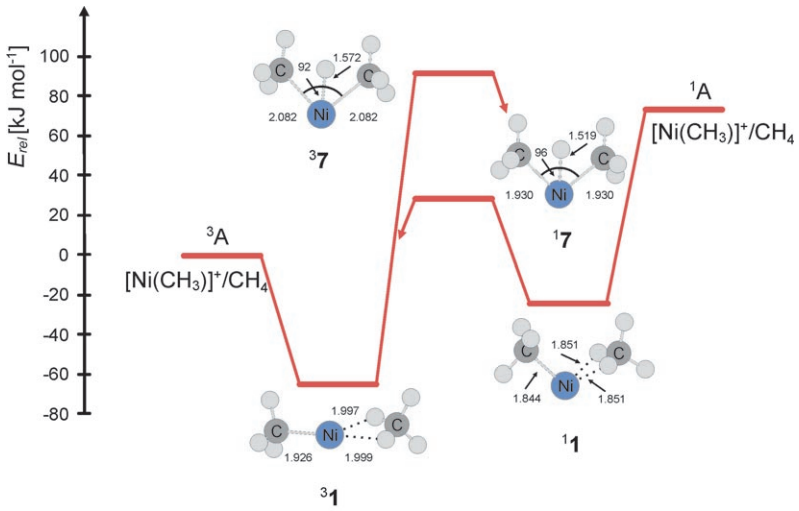

Figure 1. Schematic half-reaction profiles for the σ-CAM reactions of $[Ni(CH_3)]^+/CH_4$ in the ^{1}A and ^{3}A states of the cation.

change with methane and, according to the DFT calculations, it is the OA/RE mechanism that is energetically superior to the σ-CAM variant. Actually, for the Ru and Rh systems in their high-spin states, a σ-CAM mechanism has been identified; however, as shown in Table 3 and schematically in Figure 2 for the $[Ru(CH_3)]^+/CH_4$ couple, this rather energy-demanding process is not likely to play a role in the experiments. For the $[Ru(CH_3]^+/CH_4$ couple, this variant is also accessible for the ^3A state but is higher in energy than the OA/RE mechanism. The palladium complex deviates somehow in that both the OA/RE and the σ-CAM variants involve the ^1A low-spin ground state of $[Pd(CH_3)]^+$ with a small energetic preference for the former, at least at the B3LYP level. A definitive distinction would require much more elaborate theoretical investigations,[33] for example, advanced CCSD(T) calculations employing large basis sets. Nevertheless, the fact that the transition states of both mechanisms are energetically quite close to the entrance channel of $[Pd(CH_3)]^+/CH_4$ may account for the decreased efficiency of the ligand exchange (relative to that of the Ru and Rh analogues) as well as the rather high contribution of a *direct* ligand switch. Given the shape of the energy surface, the potential well is simply not deep enough to provide ample time for an extensive backward–forward shuttle of the hydrogen/deuterium atoms in the $[Pd(CH_3)]^+/CD_4$ encounter complex.

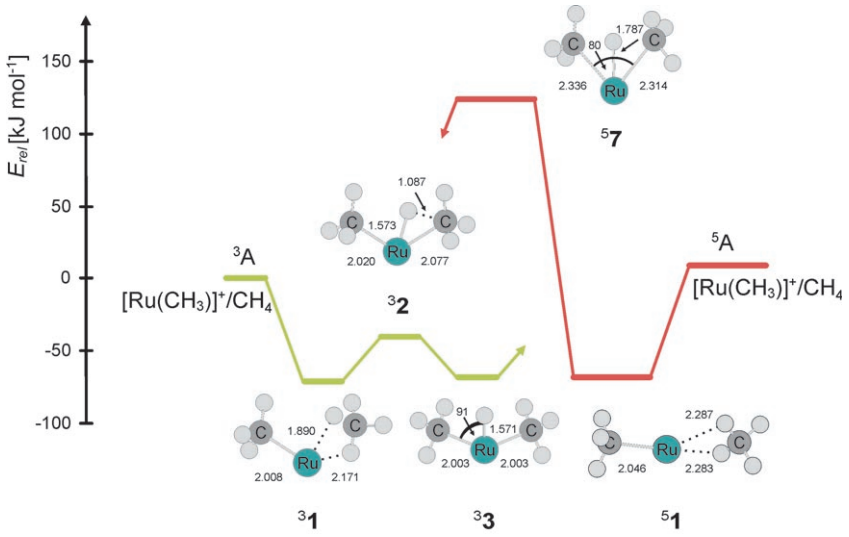

Figure 2. Schematic half-reaction profiles for the OA/RE (green) and σ-CAM (red) reactions of $[Ru(CH_3)]^+/CH_4$ in the ^3A and ^5A states of the cation.

As already stated, from the three $[M(CH_3)]^+$ complexes of the 5d transition metals M = Os, Ir, and Pt, it was only the platinum system that could be investigated experimentally (Tables 1 and 2). The fact that this complex reacts at room temperature with CH_4 at an appreciable rate and that the process is accompanied by extensive hydrogen/deuterium atom exchange in the $[Pt(CH_3)]^+/CD_4$ couple (Table 2) can be accounted for by the computational investigations (Table 3 and Figure 3). For the ^1A state, which is nearly isoenergetic with the high-spin ^3A state (as is also the case for the related $[PtH]^+$ cation[7]), all minima and transition states of the OA/RE path are located well below the entrance channel (Figure 3) and thus do not create a kinetic impediment. Furthermore, in the deep potential well of the singlet surface the trapped encounter complex has ample time to exchange the hydrogen/deuterium atoms. For the triplet state, the scenario is different in that both the transition state **2** and the insertion product **3** of an OA are located above the entrance channel. Common to either electronic state of $[Pt(CH_3)]^+$ is that a σ-CAM pathway could not be located.

As shown in Table 3, we also investigated computationally the degenerate ligand switch for the $[Os(CH_3)]^+$ and [Ir-

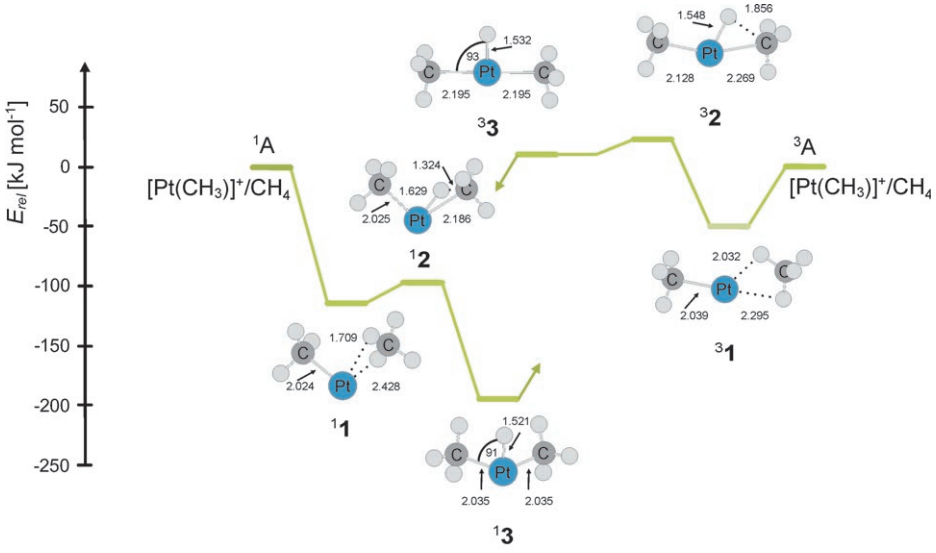

Figure 3. Schematic half-reaction profiles for the OA/RE reactions of $[Pt(CH_3)]^+/CH_4$ in the ^1A and ^3A states of the cation.

$(CH_3)]^+$ complexes. The analysis of these data reveals that if the two cations were accessible experimentally, both systems are predicted to undergo ligand exchange with methane under thermal conditions. As to the energetically preferred mechanism, for the $[Os(CH_3)]^+/CH_4$ couple we predict a TSR scenario because the ^5A ground state, close to the entrance channel, undergoes a spin flip to the excited low-spin ^3A PES, on which an OA/RE reaction will occur until, close to the exit channel, the system switches back to the high-spin ^5A ground state. There is no evidence for the involvement of a σ-CAM component. The same holds true for the $[Ir(CH_3)]^+/CH_4$ couple, which in the course of an OA/RE process also experiences two switches from the ^4A ground state to a ^2A low-spin state and then back to the ^4A state.

Conclusion

In a combined experimental/computational gas-phase study various mechanistic aspects of the degenerate ligand exchange in $[M(CH_3)]^+/CH_4$ couples have been addressed for M = Fe, Co, Ni, Ru, Rh, Pd, Os, Ir, and Pt. In line with earlier notions,[7] for the late 5d systems an OA/RE mechanism is operative. For the $[Pt(CH_3)]^+/CH_4$ couple, the reaction is confined to the singlet state; in contrast, for the complexes containing M = Os and Ir, the OA/RE variant is entangled with a TSR scenario such that close to the entrance and exit channels, the system switches from the high-spin ground to the excited low-spin states. σ-CAM mechanisms are not operative for any of the 5d complexes investigated. In contrast, for the 3d congeners with M = Fe, Co, and Ni, it is this very mechanism which is favored energetically over the OA/RE variant. Although the Fe and Co systems do not bring about thermal ligand exchange due to energetically rather demanding transition structures, in the rather inefficient reaction of the $[Ni(CH_3)]^+/CH_4$ couple a σ-CAM reaction occurs that involves two spin states. The ligand exchange commences and finishes at the high-spin triplet surface, but the actual bond activation takes place at the excited singlet state (TSR scenario). For none of the three 3d complexes do OA/RE variants play a role in either their high- or low-spin states. Finally, for the 4d systems with M = Ru, Rh, and Pd, yet another situation has been uncovered. For the ruthenium and rhodium complexes, the OA/RE mechanism is feasible energetically, and for these two couples the ligand switch is confined to their low-spin electronic states. In contrast, for the $[Pd(CH_3)]^+/CH_4$ couple, in the ^1A ground-state PES both the OA/RE and the σ-CAM mechanisms are energetically comparable, as noted earlier for the related $[Pd(H)]^+/CH_4$ complex.[5f] Although a quantitative correlation of the computational findings with the experimental data has not been intended in the present study, trends in reactivity or in the details of the reaction, for example, hydrogen-scrambling versus direct ligand switch, can be accounted for in qualitative terms by the computational results.

Acknowledgements

Financial support by the Deutsche Forschungsgemeinschaft, the Fonds der Chemischen Industrie, and the Cluster of Excellence "Unifying Concepts in Catalysis", sponsored by the Deutsche Forschungsgemeinschaft and administered by the Technische Universität Berlin, is appreciated. We are grateful to Dr. Xinhao Zhang for computational contributions.

[1] a) C. Hall, R. N. Perutz, *Chem. Rev.* **1996**, *96*, 3125; b) R. H. Crabtree, *The Organometallic Chemistry of Transition Metals*, Wiley, New York, **2001**.
[2] R. N. Perutz, S. Sabo-Etienne, *Angew. Chem.* **2007**, *119*, 2630; *Angew. Chem. Int. Ed.* **2007**, *46*, 2578, and references therein.
[3] a) C. A. Coulson, *Rev. Mod. Phys.* **1960**, *32*, 170; b) R. Hoffmann, *Angew. Chem.* **1982**, *94*, 725; *Angew. Chem. Int. Ed. Engl.* **1982**, *21*, 711; c) R. Hoffmann, *Am. Sci.* **2003**, *91*, 9; d) R. Hoffmann, S. Shaik, P. C. Hiberty, *Acc. Chem. Res.* **2003**, *36*, 750; e) G. Frenking, A. Krapp, *J. Comput. Chem.* **2007**, *28*, 15; f) S. Shaik, *New J. Chem.* **2007**, *31*, 2015; g) G. Frenking, S. Shaik, *J. Comput. Chem.* **2007**, *28*, 1; h) S. Shaik, *J. Comput. Chem.* **2007**, *28*, 51.
[4] a) "Transition State Modeling for Catalysis": S. Niu, D. L. Strout, S. Zarić, C. A. Bayse, M. B. Hall, *ACS Symp. Ser.* **1998**, *721*, 138; b) S. Niu, M. B. Hall, *Chem. Rev.* **2000**, *100*, 353; c) H. Heiberg, O. Gropen, O. Swang, *Int. J. Quantum Chem.* **2003**, *92*, 391; d) S. Sakaki, *Top. Organomet. Chem.* **2005**, 12, 31.
[5] a) T. J. Carlin, L. Sallans, C. J. Cassady, D. B. Jacobson, B. S. Freiser, *J. Am. Chem. Soc.* **1983**, *105*, 6320; b) L. F. Halle, F. S. Klein, J. L. Beauchamp, *J. Am. Chem. Soc.* **1984**, *106*, 2543; c) Q. Zhang, M. T. Bowers, *J. Phys. Chem. A* **2004**, *108*, 9755; d) D. Schröder, H. Schwarz, *Can. J. Chem.* **2005**, *83*, 1936; e) M. Schlangen, D. Schröder, H. Schwarz, *Angew. Chem.* **2007**, *119*, 1667; *Angew. Chem. Int. Ed.* **2007**, *46*, 1641; f) M. Schlangen, H. Schwarz, *Angew. Chem.* **2007**, *119*, 5711; *Angew. Chem. Int. Ed.* **2007**, *46*, 5614.
[6] a) D. Schröder, S. Shaik, H. Schwarz, *Acc. Chem. Res.* **2000**, *33*, 139; b) R. Poli, J. N. Harvey, *Chem. Soc. Rev.* ***2003***, *32*, 1; c) H. Schwarz, *Int. J. Mass Spectrom.* **2004**, *237*, 75; d) J. M. Mercero, J. M. Matxain, X. Lopez, D. M. York, A. Largo, L. A. Erikson, J. M. Ugalde, *Int. J. Mass Spectrom.* **2005**, *240*, 37; e) I. Rivalta, N. Russo, E. Sicilia, *J. Comput. Chem.* **2006**, *27*, 174; f) B. K. Carpenter, *Chem. Soc. Rev.* **2006**, *35*, 736; g) J. N. Harvey, *Phys. Chem. Chem. Phys.* **2007**, *9*, 331; h) S. Shaik, H. Hirao, D. Kumar, *Acc. Chem. Res.* **2007**, *40*, 532.
[7] a) G. Ohanessian, M. J. Brusich, W. A. Goddard III, *J. Am. Chem. Soc.* **1990**, *112*, 7179; b) G. Ohanessian, W. A. Goddard III, *Acc. Chem. Res.* **1990**, *23*, 386; c) X.-G. Zhang, R. Liyanage, P. B. Armentrout, *J. Am. Chem. Soc.* **2001**, *123*, 5563.
[8] a) P. Pyykkö, *Chem. Rev.* **1988**, *88*, 563; b) H. Schwarz, *Angew. Chem.* **2003**, *115*, 4580; *Angew. Chem. Int. Ed.* **2003**, *42*, 4442.
[9] R. Hoffmann, *The Same and Not the Same*, Columbia University Press, New York, **1995**.
[10] W. H. Lam, G. Jia, Z. Liu, C. P. Lan, O. Eisenstein, *Chem. Eur. J.* **2003**, *9*, 2775.
[11] M. Armélin, Diploma Thesis, Technische Universität Berlin, **2007**.
[12] K. Eller, H. Schwarz, *Int. J. Mass Spectrom. Ion Processes* ***1989***, *93*, 243.
[13] S. Maruyama, L. R. Anderson, R. E. Smalley, *Rev. Sci. Instrum.* ***1990***, *61*, 3686.
[14] M. Engeser, T. Weiske, D. Schröder, H. Schwarz, *J. Phys. Chem. A* **2003**, *107*, 2855.
[15] R. A. Forbes, F. H. Laukien, J. Wronka, *Int. J. Mass Spectrom. Ion Processes* **1988**, *83*, 23.
[16] a) D. B. Jacobson, B. S. Freiser, *J. Am. Chem. Soc.* **1984**, *106*, 3891; b) P. B. Armentrout, R. Georgiadis, *Polyhedron*, **1988**, *7*, 1573; c) E. R. Fisher, L. S. Sunderlin, P. B. Armentrout, *J. Phys. Chem.* **1989**, *93*, 7375.
[17] a) J. Schwarz, C. Heinemann, D. Schröder, H. Schwarz, J. Hrušák, *Helv. Chim. Acta* **1996**, *79*, 1; b) J. Schwarz, D. Schröder, H. Schwarz, C. Heinemann, J. Hrušák *Helv. Chim. Acta* **1996**, *79*, 1110.

[18] D. Schröder, H. Schwarz, D. E. Clemmer, Y.-M. Chen, P. B. Armentrout, V. I. Baranov, D. K. Böhme, *Int. J. Mass Spectrom. Ion Processes* **1997**, *161*, 175.
[19] a) F. Nakao, *Vacuum* **1975**, *25*, 431; b) J. E. Bartmess, R. M. Georgiadis, *Vacuum*, **1983**, *33*, 149.
[20] a) T. Su, M. T. Bowers, *Int. J. Mass Spectrom. Ion Phys.* **1973**, *12*, 347; b) T. Su, E. C. F. Su, M. T. Bowers, *J. Chem. Phys.* **1978**, *69*, 2243.
[21] D. Schröder, T. Weiske, H. Schwarz, *Int. J. Mass Spectrom.* **2002**, *219*, 729.
[22] a) N. Tsierkezos, D. Schröder, H. Schwarz, *J. Phys. Chem. A* **2003**, *107*, 9575; b) M. Schlangen, D. Schröder, H. Schwarz, *Chem. Eur. J.* **2007**, *13*, 6810.
[23] a) D. Schröder, T. Weiske, M. Brönstrup, C. Daniel, J. Spandl, H. Hartl, *Int. J. Mass Spectrom.* **2003**, *228*, 743; b) D. Schröder, H. Schwarz, S. Schenk, E. Anders, *Angew. Chem.* **2003**, *115*, 5241; *Angew. Chem. Int. Ed.* **2003**, *42*, 5087; c) J. Roithová, J. Hrušák, D. Schröder, H. Schwarz, *Inorg. Chim. Acta* **2005**, *358*, 4287; d) S. Feyel, D. Schröder, H. Schwarz, *J. Phys. Chem. A* **2006**, *110*, 2647; e) D. Schröder, J. Roithová, H. Schwarz, *Int. J. Mass Spectrom.* **2006**, *254*, 197; f) J. Roithová, D. Schröder, *Phys. Chem. Chem. Phys.* **2007**, *9*, 731.
[24] a) C. Lee, W. Yang, R. G. Parr, *Phys. Rev. B* **1988**, *37*, 785; b) A. D. Becke, *J. Chem. Phys.* **1993**, *98*, 5648.
[25] Gaussian 03, Revision C.02, M. J. Frisch, G. W. Trucks, H. B. Schlegel, G. E. Scuseria, M. A. Robb, J. R. Cheeseman, J. A. Montogmery, Jr., T. Vreven, K. N. Kudin, J. C. Burant, J. M. Millam, S. S. Iyengar, J. Tomasi, V. Barone, B. Mennucci, M. Cossi, G. Scalmani, N. Rega, G. A. Petersson, H. Nakatsuji, M. Hada, M. Ehara, K. Toyota, R. Fukuda, J. Hasegawa, M. Ishida, T. Nakajima, Y. Honda, O. Kitao, H. Nakai, M. Klene, X. Li, J. E. Knox, H. P. Hratchian, J. B. Cross, V. Bakken, C. Adamo, J. Jaramillo, R. Gomperts, R. E. Stratmann, O. Yazyev, A. J. Austin, R. Cammi, C. Pomelli, J. W. Ochterski, P. Y. Ayala, K. Morokuma, G. A. Voth, P. Salvador, J. J. Dannenberg, V. G. Zakrezewski, S. Dapprich, A. D. Daniels, M. C. Strain, O. Farkas, D. K. Malick, A. D. Rabuck, K. Raghavachari, J. B. Foresman, J. V. Ortiz, Q. Cui, A. G. Baboul, S. Clifford, J. Cioslowski, B. B. Stefanov, G. Liu, A. Liashenko, P. Piskorz, I. Komaromi, R. L. Martin, D. J. Fox, T. Keith, M. A. Al-Laham, C. Y. Peng, A. Nanayakkara, M. Challacombe, P. M. W. Gill, B. Johnson, W. Chen, M. W. Wong, C. Gonzalez, J. A. Pople, Gaussian, Inc., Wallingford CT, **2004**.
[26] a) A. Schäfer, H. Horn, R. Ahlrichs, *J. Chem. Phys.* **1992**, *97*, 2571; b) A. Schäfer, C. Huber, R. Ahlrichs, *J. Chem. Phys.* **1994**, *100*, 5829.
[27] A. J. H. Wachters, *J. Chem. Phys.* **1970**, *52*, 1033.
[28] a) D. Andrae, U. Haeussermann, M. Dolg, H. Stoll, H. Preuss, *Theor. Chim. Acta* **1990**, *77*, 123; b) M. Dolg, H. Stoll, H. Preuss, R. M. Pitzer, *J. Phys. Chem.* **1993**, *97*, 5852; c) K. A. Peterson, D. Figgen, M. Dolg, H. Stoll, *J. Chem. Phys.* **2007**, *126*, 124101.
[29] a) K. Fukui, *J. Phys. Chem.* **1970**, *74*, 4161; b) K. Fukui, *Acc. Chem. Res.* **1981**, *14*, 363; c) C. Gonzales, H. B. Schlegel, *J. Phys. Chem.* **1990**, *94*, 5523.
[30] H. Heiberg, L. Johansson, O. Gropen, O. B. Ryan, O. Swang, M. Tilset, *J. Am. Chem. Soc.* **2000**, *122*, 10831.
[31] a) J. Loos, D. Schröder, W. Zummack, H. Schwarz, R. Thissen, O. Dutuit, *Int. J. Mass Spectrom.* **2002**, *214*, 105; b) C. Trage, D. Schröder, H. Schwarz, *Organometallics* **2003**, *22*, 693; c) M. Schlangen, D. Schröder, H. Schwarz, *Helv. Chim. Acta* **2005**, *88*, 1405; d) B. Butschke, M. Schlangen, H. Schwarz, D. Schröder, *Z. Naturforsch. B* **2007**, *62*, 309; e) J. Roithová, D. Schröder, *J. Am. Chem. Soc.* **2007**, *129*, 15314.
[32] a) J. B. Schilling, W. A. Goddard III, J. L. Beauchamp, *J. Am. Chem. Soc.* **1987**, *109*, 5573; b) C. W. Bauchschlicher, Jr., S. R. Langhoff, H. Partridge, L. A. Barnes, *J. Chem. Phys.* **1989**, *91*, 2399; c) M. C. Holthausen, C. Heinemann, H. H. Cornehl, W. Koch, H. Schwarz, *J. Chem. Phys.* **1995**, *102*, 4931.
[33] a) "Transition State Modeling for Catalysis" (Eds.: D. G. Truhlar, K. Morokuma), *ACS Symp. Ser.* **1998**, *721*; b) W. Koch, M. C. Holthausen, *A Chemist's Guide to Density Functional Theory*, Wiley-VCH, Weinheim, **2000**; c) *Computational Organometallic Chemistry* (Ed.: T. R. Cundari), Marcel Dekker, New York, **2001**; d) P. Schreiner, *Angew. Chem.* **2007**, *119*, 4295; *Angew. Chem. Int. Ed.* **2007**, *46*, 4217; e) S. Feyel, J. Döbler, R. Höckendorf, M. K. Beyer, J. Sauer, H. Schwarz, *Angew. Chem.* **2008**, *120*, 1972; *Angew. Chem. Int. Ed.* **2008**, *47*, 1946; f) For a recent, thorough discussion, see: Y. Zhao, D. G. Truhlar, *Acc. Chem. Res.* **2008**, *41*, 157.

Received: January 8, 2008
Published online: April 24, 2008

